



Project: Radiation protection and the safety of Radiation Sources

INTEREST – INTERnational REMote Student Training at JINR

Wave 6

Student:

Jelena Vlahović

Faculty of Sciences, University of Novi Sad

Supervisor:

Dr Said AbouElazm

Dzhelepov Laboratory of Nuclear Problems

14 February – 25 March, 2022

Radiation Protection and Dosimetry

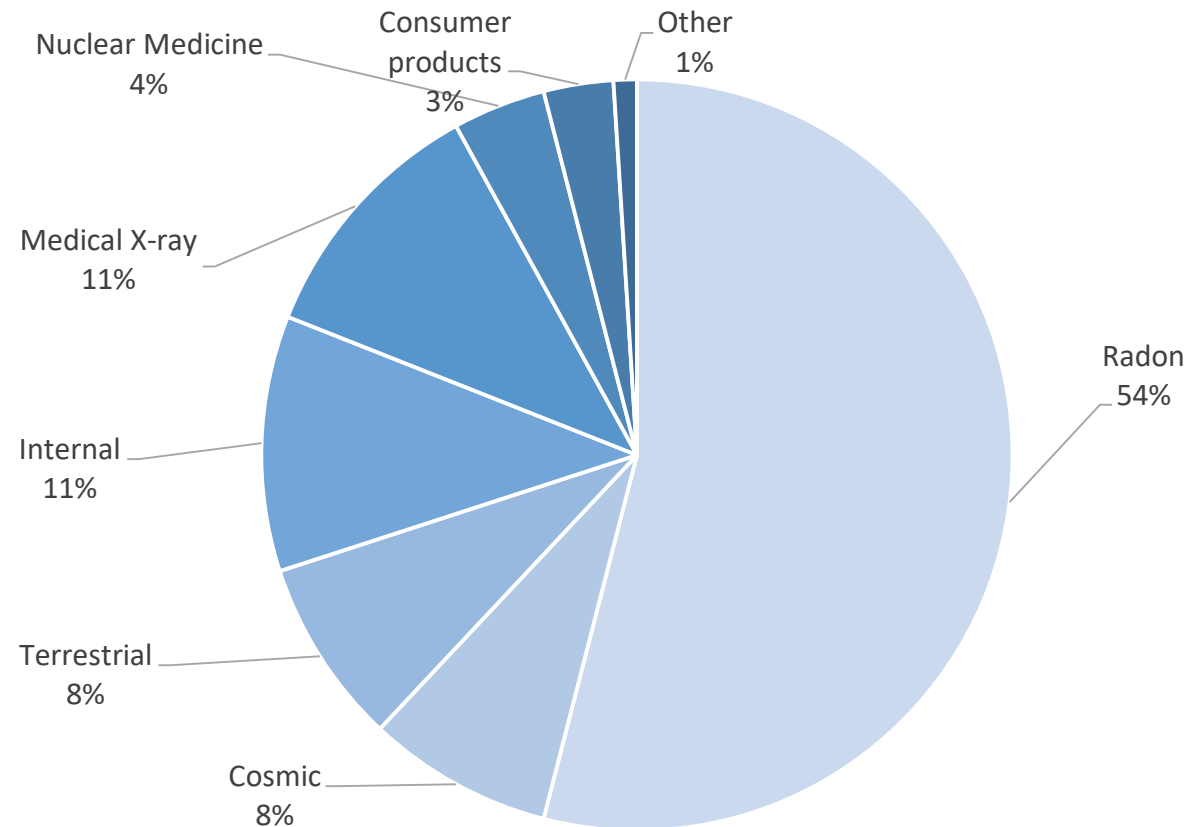


Figure 1. Sources of radiation exposure

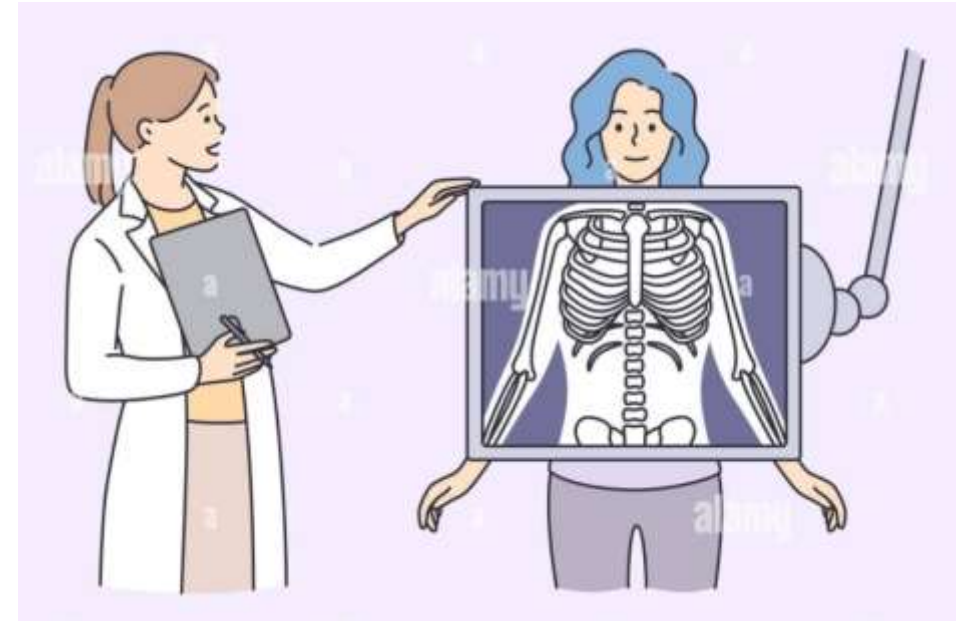


Figure 2. Types of radiation exposure

Types of radiation exposure:

1. External
2. Internal → inhalation and ingestion

Radiation Protection and Dosimetry

Absorbed dose

Energy deposited in a kilogram of a substance by the radiation.

$$D = \frac{d\varepsilon}{dm} \quad [Gy = \frac{J}{kg}]$$

Equivalent dose

Absorbed dose weighted for harmful effects of different radiations (radiation weighting factor Q).

$$H = D * Q * N \quad [Sv]$$

Effective dose

Equivalent dose weighted for susceptibility to harm different tissues (tissue weighting factor W_i).

$$H_i = \Sigma W_i H_i$$

Scintillation detectors

Scintillation material → produce scintillation of light when ionizing radiation passes through them.

There are two commonly used types of scintillators, inorganic crystals and organic scintillators.

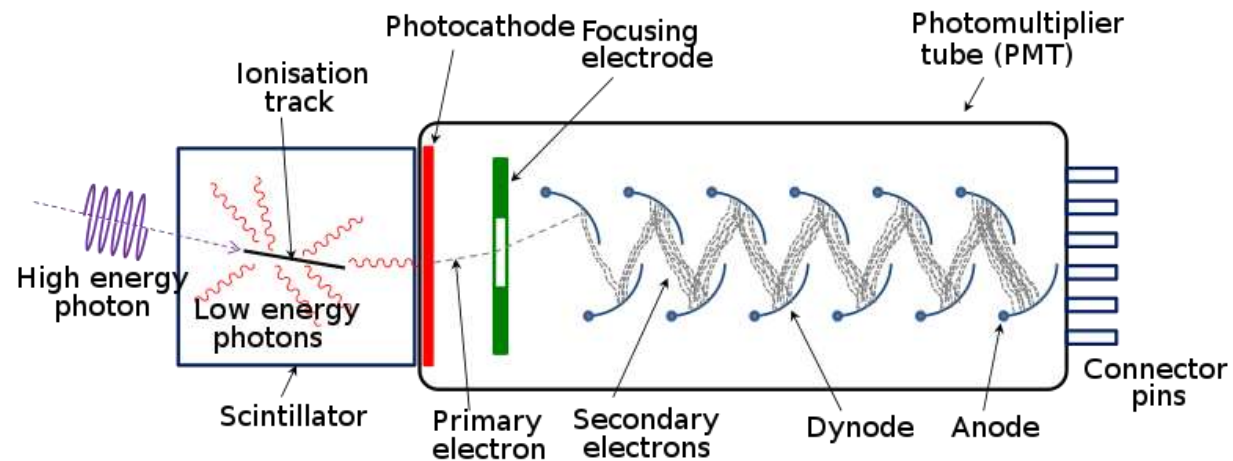


Figure 3. A photomultiplier tube scheme

Inorganic scintillators:

BGO – Bismuth Germanate ($\text{Bi}_4\text{Ge}_3\text{O}_{12}$)

- High Z
- High density
- Good photopeak to Compton ratio
- Applications: *PET, HEP, NP, space and medical physics*
- Highly effective γ -ray absorber

NaI (Tl) – Sodium Iodide (Tl)

- High light output
- Available in single-crystal and polycrystalline form
- Applications: *TOF measurements, Positron lifetimes studies, PET, HEP and NP*

Basic properties of scintillating crystals

Scintillator	Light output	Decay (ns)	Wavelength (nm) max	Density (g/cm ³)	Hygroscopic
Na(Tl)	100	250	415	3.67	yes
CsI	5	16	315	4.51	slightly
BGO	20	300	480	7.13	no
BaF ₂ (f/s)	3/16	0.7/630	220/310	4.88	slightly
CaF ₂	50	940	435	3.18	no
CdWO ₄	40	14000	475	7.9	no
LaBr ₃ (Ce)	165	16	380	5.29	yes
LYSO	75	41	420	7.1	no
YAG(Ce)	15	70	550	4.57	no

Na(Tl)



BGO



Experimental set-up

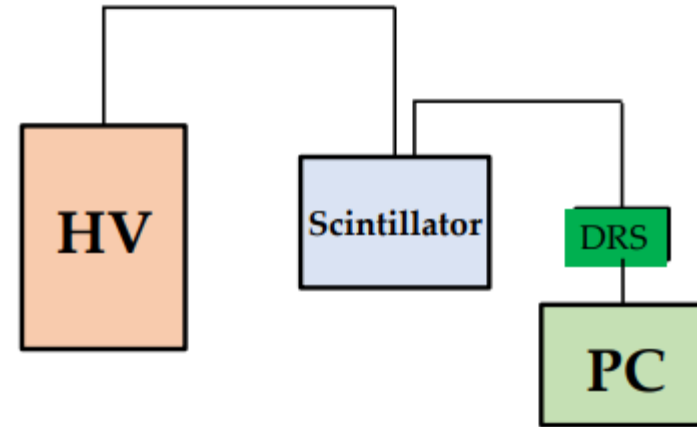
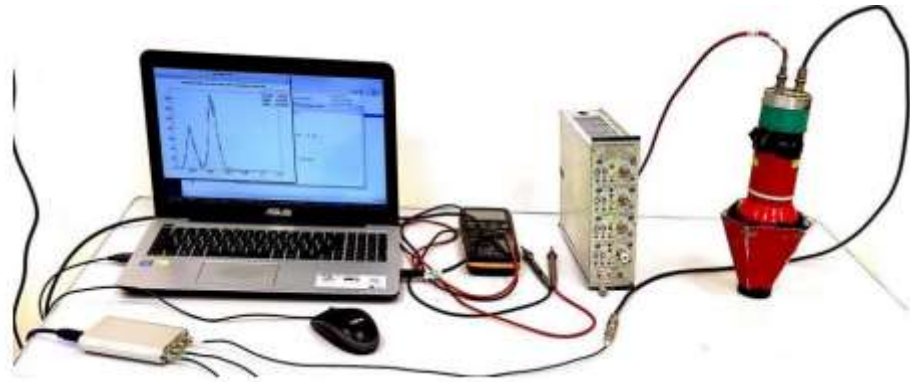


Figure 4. Laboratory and experimental set-up

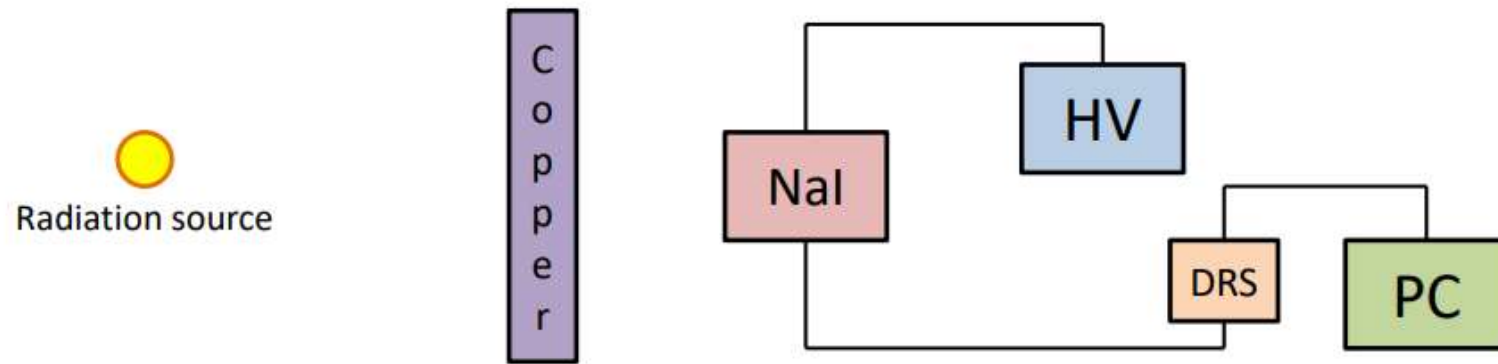
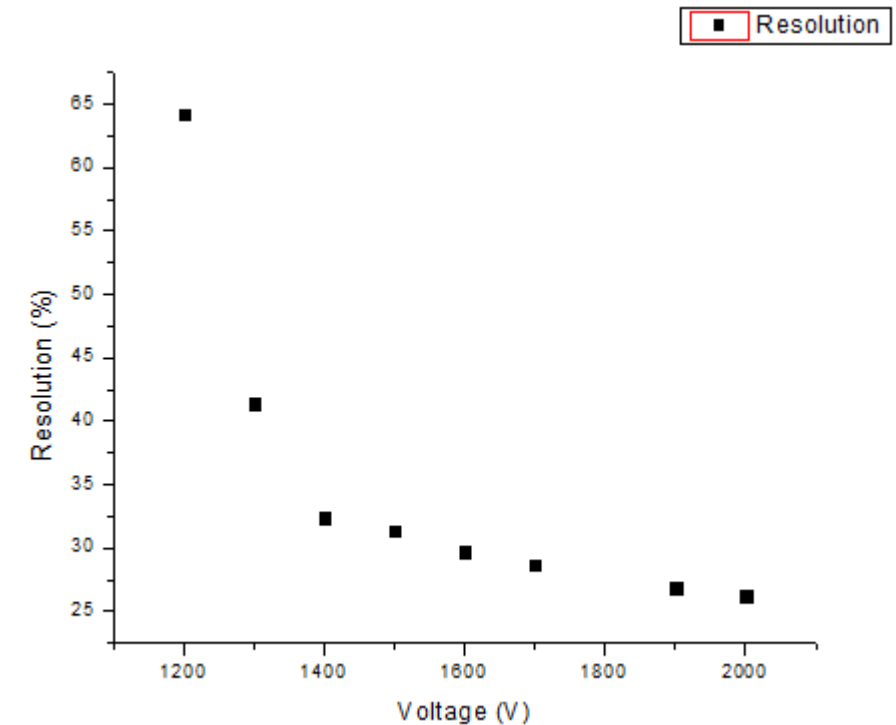


Figure 5. Experimental set-up used to determine the attenuation coefficient

Task 1.1. The relation between the resolution and the applied voltage for BGO detector

$$R = \frac{\text{Sigma}}{\text{Mean}} * 2.35$$

Voltage [V]	Sigma	Mean	R [%]
1200	0.4436	1.624	64.2
1300	0.237	1.345	41.4
1400	0.2649	1.92	32.4
1500	0.4004	3	31.4
1600	0.5583	4.418	29.7
1700	0.7485	6.121	28.7
1900	1.225	10.7	26.9
2000	1.53	13.7	26.2



*Figure 6. The relation between the resolution and the applied voltage for **BGO** scintillation detector*

Task 1.2. Energy calibration for BGO

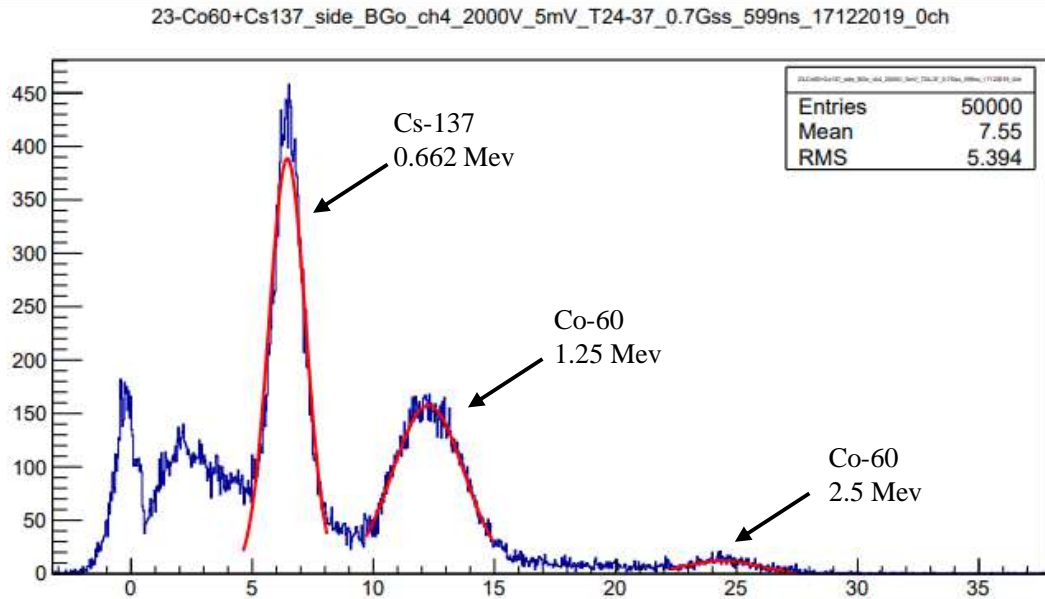


Figure 7. Cs-137 and Co-60 spectrum from measurements with BGO detector at 2000V

Equation of calibration:

$$y = 0,03553 + 9,74465 * x$$

where

y= PMT signal A.U.

x= energy of the unknown source

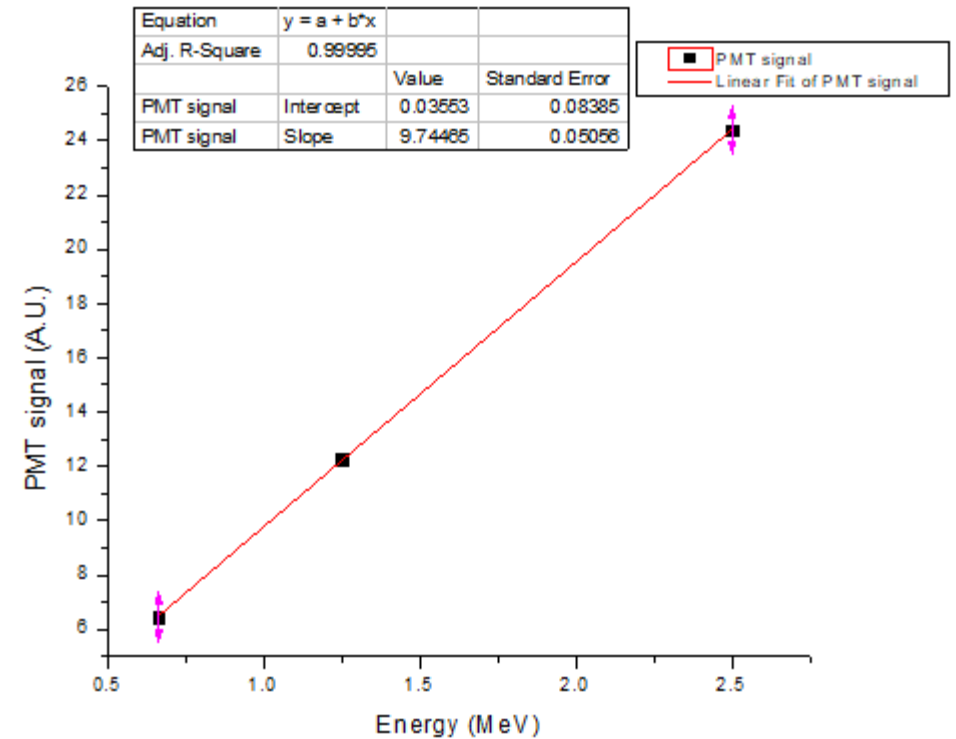


Figure 8. Energy calibration function

Task 2.1. The relation between the resolution and the applied voltage for NaI detector

$$R = \frac{\text{Sigma}}{\text{Mean}} * 2,35$$

Voltage [V]	Sigma	Mean	R [%]
900	0.6135	23.68	6.09
1000	0.95656	40.65	5.53
1100	1.514	65.79	5.41
1200	1.998	98.75	4.75
1300	2.562	137.4	4.38

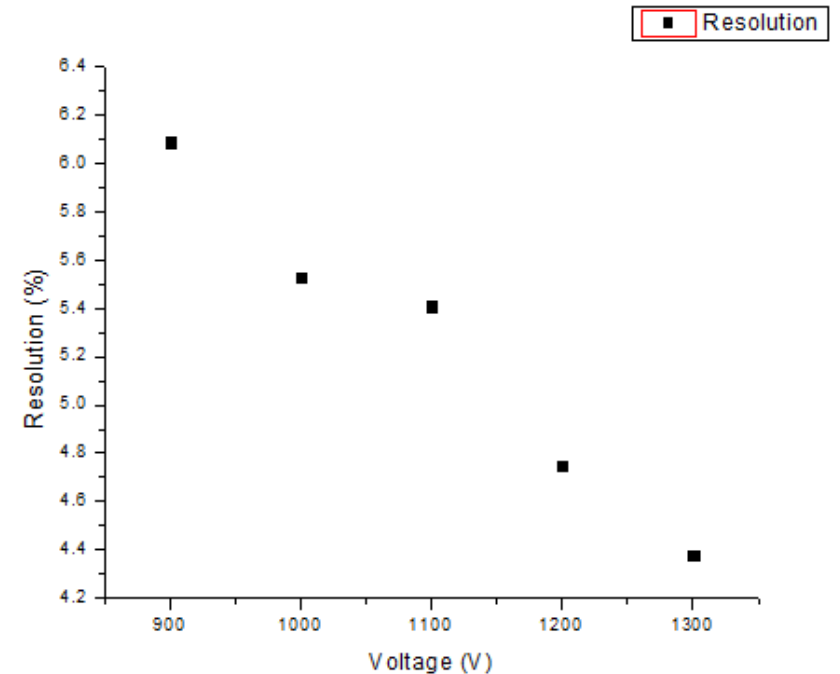


Figure 9. The relation between the resolution and the applied voltage for NaI scintillation detector

Task 2.2. Energy calibration for NaI

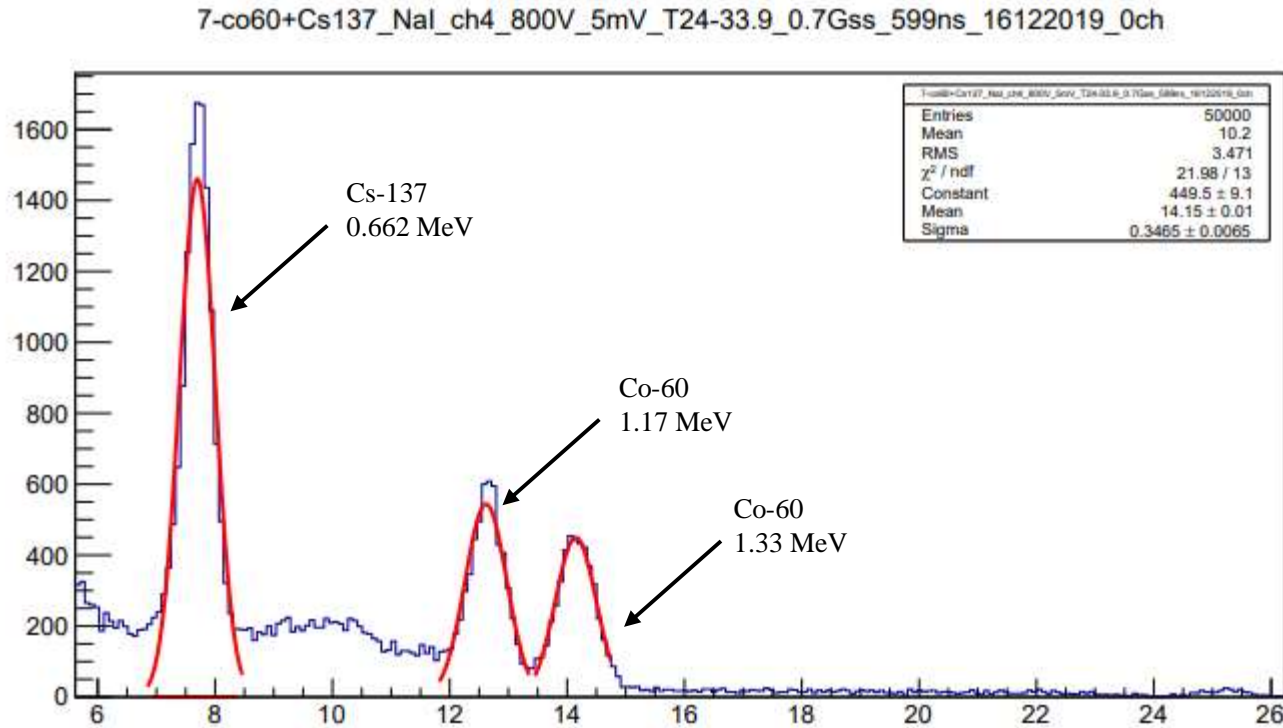


Figure 10. Cs-137 and Co-60 spectrum from measurements with NaI detector at 800V

Equation of calibration:

$$y = 1,30501 + 9,66072 * x$$

where

y= PMT signal A.U.

x= energy of the unknown source

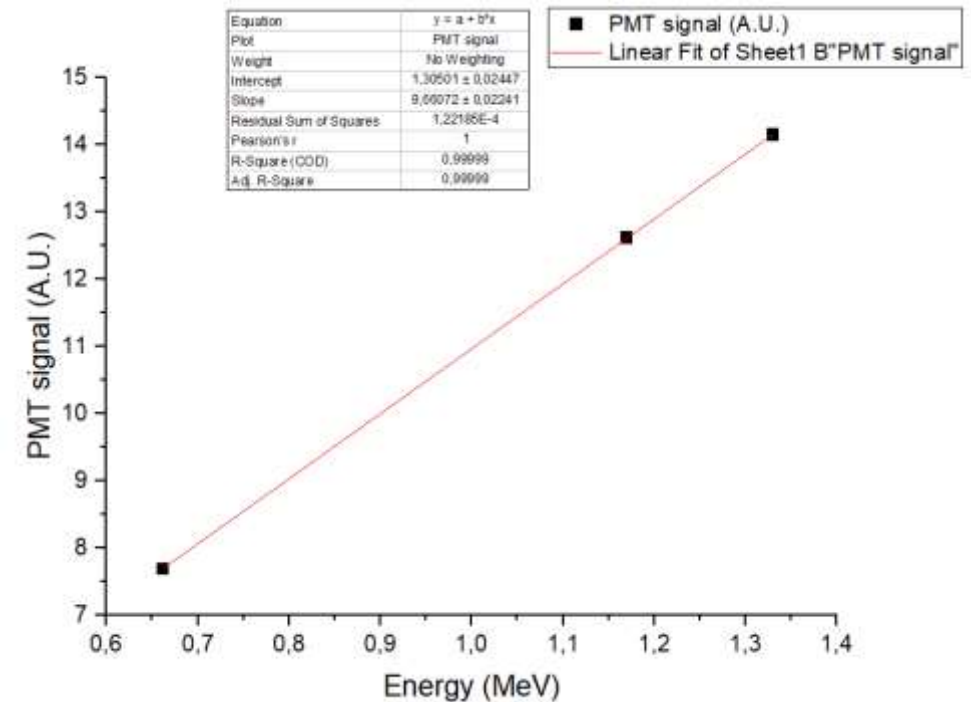


Figure 11. Energy calibration function

Task 2.3. Identification of unknown sources

- The energy of each peak was determined using the linear energy calibration curve.
- Equation calibration curve for BGO detector:

$$y = 0,03553 + 9,74465 * x$$

x - Energy of the unknown source
 y – PMT signal

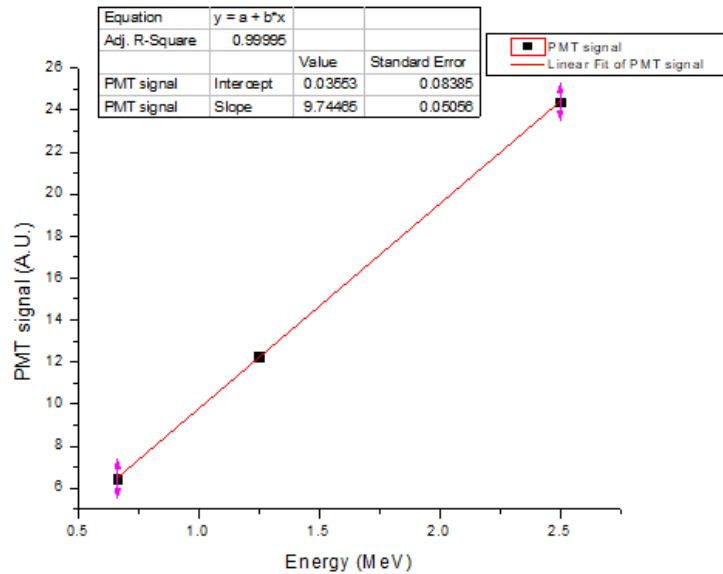


Figure 12. Energy calibration function

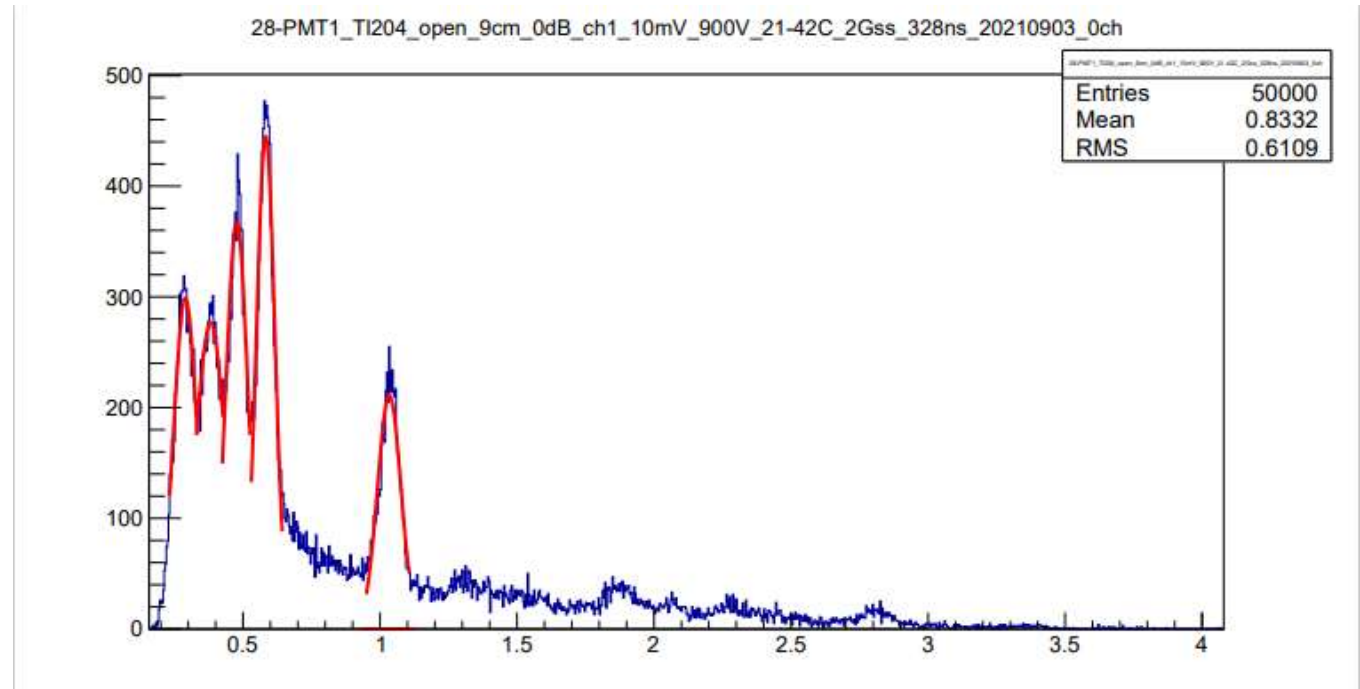


Figure 13. Spectre of unknown radioactive source

Peak 1 → Ba-140 or Mg-28 26,07 keV

Peak 2 → I-125 or Te-125m 35,49 keV

Peak 3 → Pb-210 or Rh-124m 45,34 keV

Peak 4 → Te-127m or Am-241 56,14 keV

Peak 5 → Sm-153 or Sm-155 102,43 keV

Task 2.3. Identification of unknown sources

- Equation calibration curve for NaI detector:
$$y = 1,30501 + 9,66072 * x$$

x - Energy of the unknown source
y – PMT signal

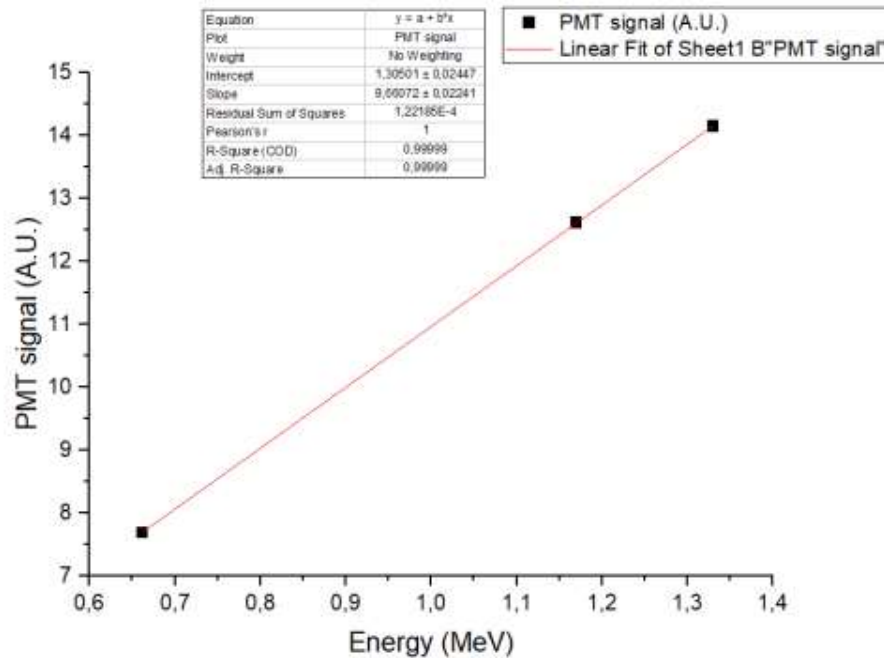


Figure 14. Energy calibration function

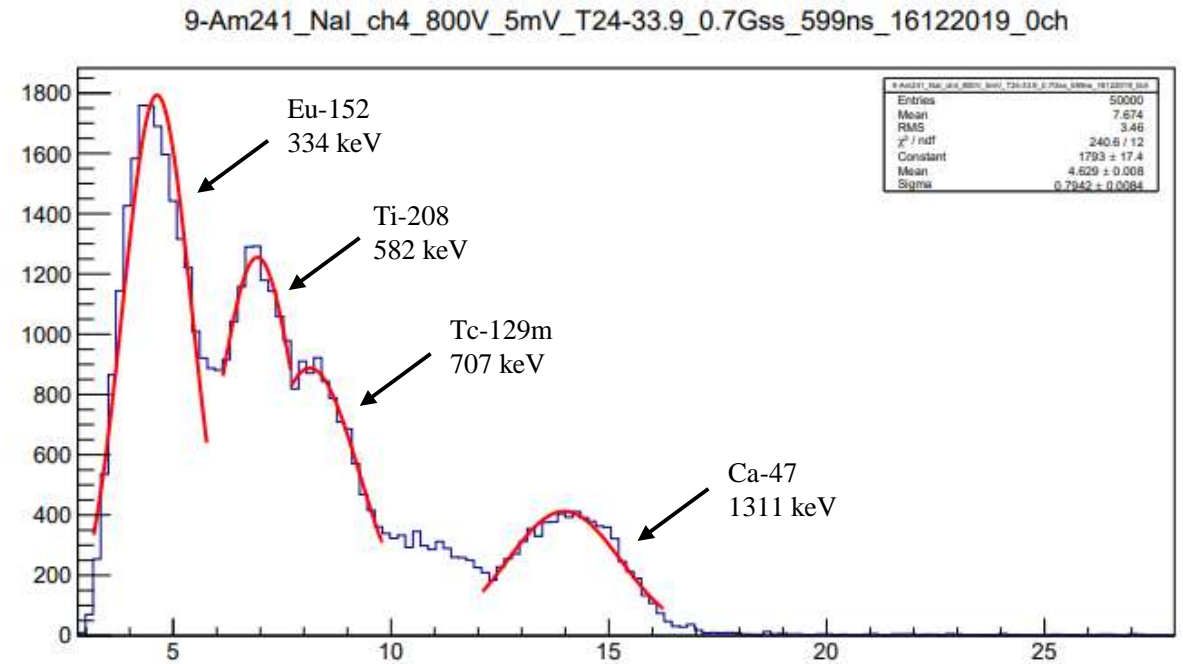


Figure 15. Spectre of unknown radioactive source

Task 3. Attenuation of γ radiation as a function of thickness and atomic number Z

- Attenuation coefficient describes the fraction of beam that is absorbed or scattered per unit thickness of the absorber.

$$I = I_0 e^{-\mu x}$$

where μ is the attenuation coefficient.

- The mass attenuation coefficient of a material is the attenuation coefficient normalized by the density of the material.

$$\mu_m = \frac{\mu}{\rho}$$

Task 3. Attenuation of γ radiation as a function of thickness and atomic number Z

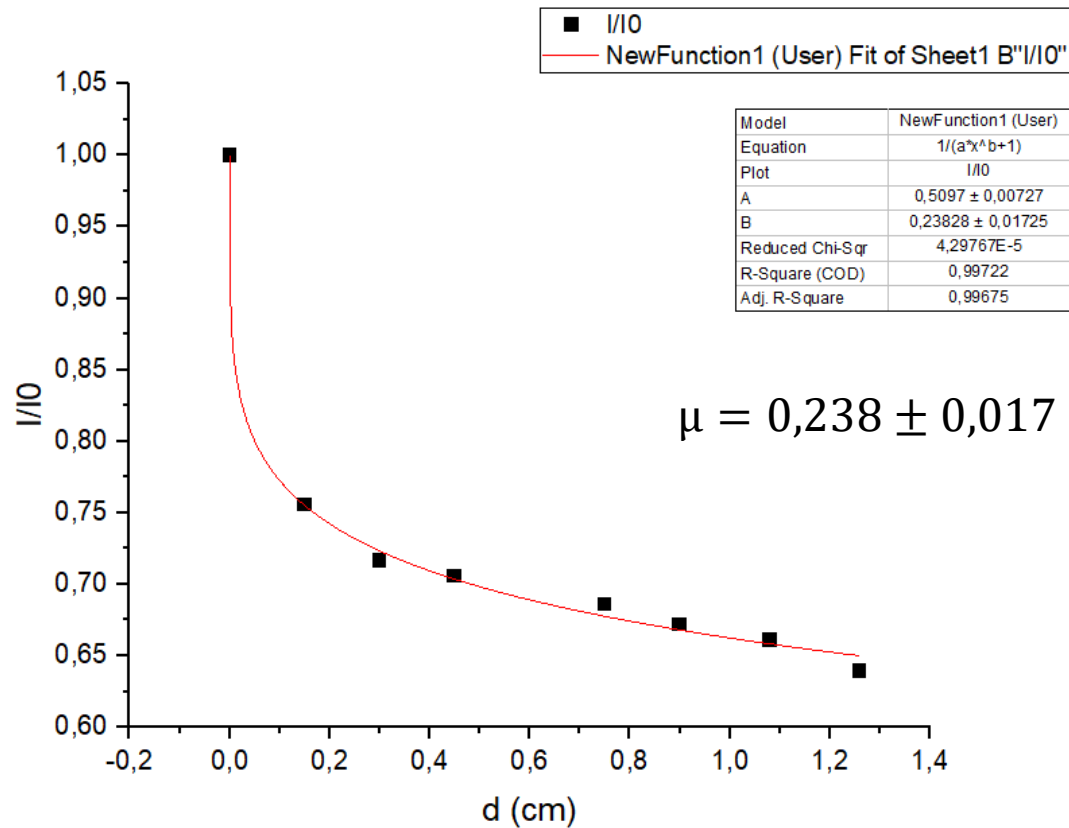


Figure 16. Determination of attenuation coefficient for *Al*

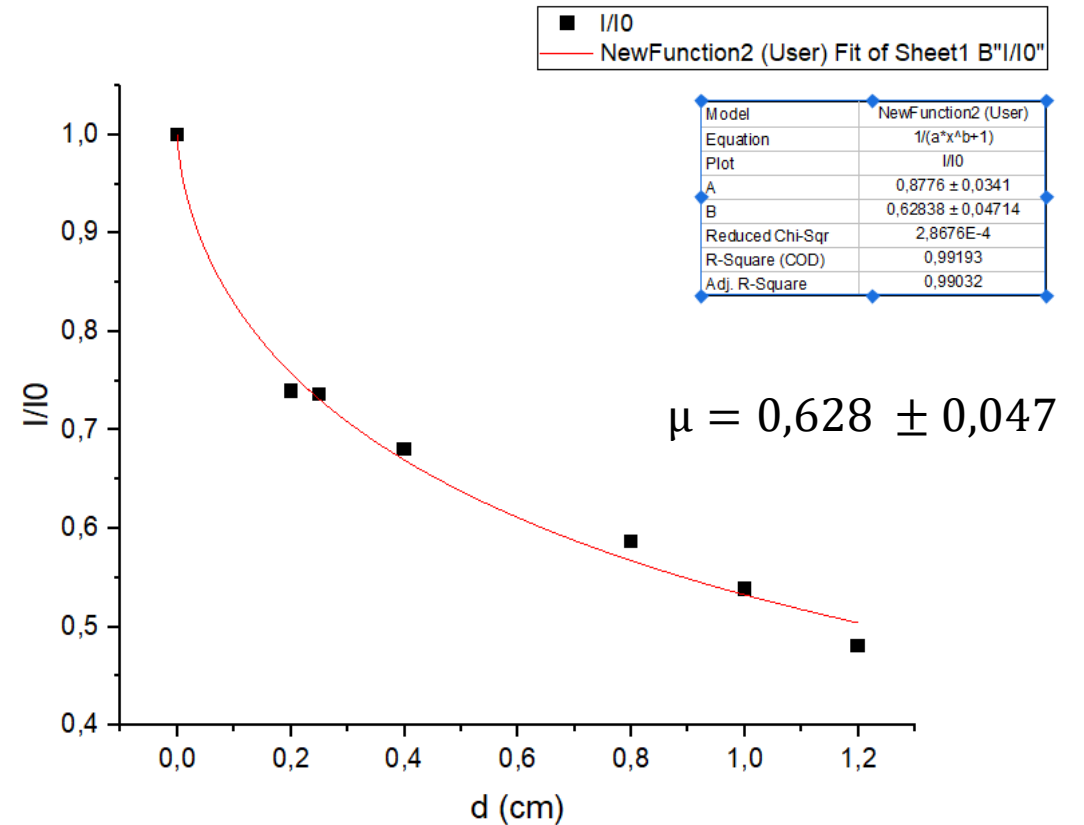


Figure 17. Determination of attenuation coefficient for *Cu*

Task 4. The range of α -particles in the air

- We used a plastic detector to determine the range of alpha particles in air.
- The source we used in this case was ^{239}Pu with the energy of alpha particles being 5 MeV.
- The applied voltage was 2000V.

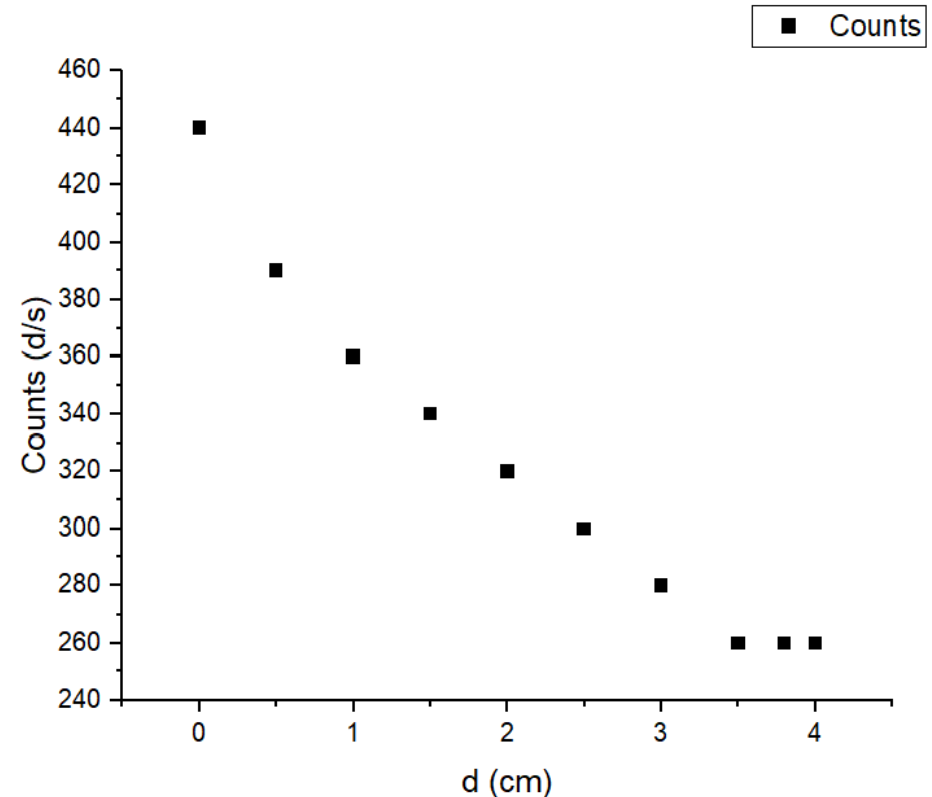
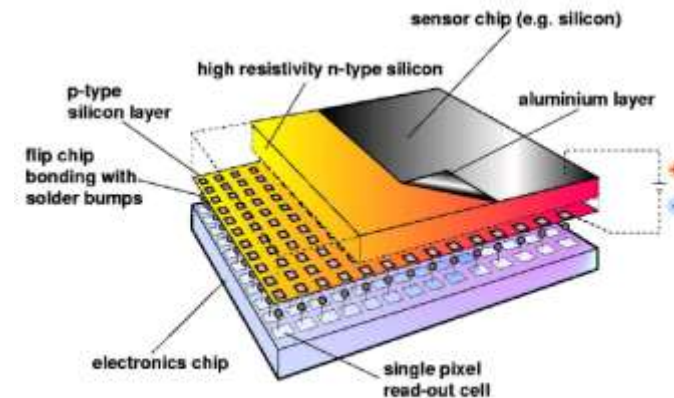


Figure 18. The range of α -particles in air

Pixel Detectors

Characteristics of pixel detectors:

- Advanced detectors, like a digital camera.
- They consist out of **3 parts**:
 - Sensor (Si)
 - Electronic chip
 - USB
- The size of the sensor is 1.5x1.5cm and it has 256 x 256 pixels.
 - The pixel size is 55 μ m x 55 μ m.
- These detectors have high resolution and are used for registration of different types of radiation.
 - Such as X-ray, gamma, electron, neutron and charged particles.



Detector and electronics readout are optimized separately

Figure 19. Example of a hybrid pixel detector with its components

Conclusion

- In the case of the BGO detector, the value of resolution increases as we increase the applied voltage.
 - But, in general, BGO detectors do not possess good resolution.
- We came to the same conclusion with the NaI detector. By increasing the applied voltage we increased the resolution as well.
 - Comparing the two detectors previously mentioned, we can conclude that the NaI detector has better resolution.
- Through the process of the energy calibration of a detector we can determine the energy of an unknown source.
- According to the results we have obtained we can conclude that the attenuation coefficient increases with increasing atomic number and increasing physical density of the absorbing material.

References

1. Cember, H., Introduction to Health Physics, 3rd Edition, McGraw-Hill, New York (2000).
2. Attix, F.H., Introduction to Radiological Physics and Radiation Dosimetry, Wiley, New York (1986).
3. Martin J.E., Physics for Radiation Protection, Wiley-VCH Verlag GmbH & Co. KGaA, Weinheim (2013).
4. Knoll, G. F., Radiation detection and measurement, 4th Edition, Wiley (2010).